Original

Meyer, M.; Paetsch, J.; Geyer, B.; Thomas, H.:

Revisiting the Estimate of the North Sea Air−Sea Flux of CO2 in 2001/2002: The Dominant Role of Different Wind Data Products

In: Journal of Geophysical Research : Biogeosciences (2018) AGU

DOI: 10.1029/2017JG004281

Journal of Geophysical Research: Biogeosciences

RESEARCH ARTICLE
10.1029/2017JG004281

Key Points:
- The use of the new wind product coastDat increases the earlier estimated CO_2 uptake flux in coastal areas of the North Sea (0.72 mol C·m^{-2}·yr^{-1}) by 0.88 mol C·m^{-2}·yr^{-1}
- Comparisons with observations show that for coastal areas coastDat appears more suitable than ERA40
- In the light of ongoing ocean acidification and warming a refinement of marine pCO_2 observations bears the larger potential to reduce uncertainty of the CO_2 flux estimates than further refinement of wind products

Correspondence to:
J. Pätsch,
johannes.paetsch@uni-hamburg.de

Citation:
Meyer, M., Pätsch, J., Geyer, B., & Thomas, H. (2018). Revisiting the estimate of the North Sea air-sea flux of CO_2 in 2001/2002: The dominant role of different wind data products. *Journal of Geophysical Research: Biogeosciences*, *123*, 1511–1525. https://doi.org/10.1029/2017JG004281

Received 7 NOV 2017
Accepted 3 APR 2018
Accepted article online 12 APR 2018
Published online 9 MAY 2018

Revisiting the Estimate of the North Sea Air-Sea Flux of CO_2 in 2001/2002: The Dominant Role of Different Wind Data Products

Maybritt Meyer[1], Johannes Pätsch[1], Beate Geyer[2], and Helmuth Thomas[3]

[1]Institute of Oceanography, University of Hamburg, Hamburg, Germany, [2]Institute of Coastal Research, Helmholtz-Zentrum Geesthacht, Geesthacht, Germany, [3]Department of Oceanography, Dalhousie University, Halifax, Nova Scotia, Canada

Abstract For the North Sea, a semienclosed shelf sea in the northeastern North Atlantic, the seasonal and annual CO_2 air-sea fluxes (ASF) had been estimated for 2001 and 2002 in earlier work. The underlying observations, ΔpCO_2, salinity, and temperature had been combined with 6-hourly wind data derived from ERA40 reanalysis. In order to assess the impact of different wind data products on the computation of CO_2 ASF, we compared ERA40 wind data with coastDat data derived from the nonhydrostatic regional climate model COSMO-CLM. From the four observational months September, November, February, and May all but the May data show higher wind speeds for coastDat than for ERA40, especially off the Norwegian, UK, and continental coasts. Largest differences occur in the northern offshore areas. The comparison with observed wind data supports this feature generally: At Helgoland, an island in the German Bight, and at the Belgium pile "Westhinder" the ERA40 data underestimate both, the coastDat data and the observations. Wind observations for two Norwegian North Sea platforms were available: At the northern station "Troll" off the Norwegian coast the coastDat data overestimate the observations in winter. At "Ekofisk" in the central North Sea the ERA40 data fit the observations well, while the coastDat data slightly overestimate the observational data in all months but in May. The corresponding CO_2 ASF estimates show strongest deviations off the Norwegian coast. Using different bulk formulas for determining the net annual ASF resulted in differences due to different wind products of up to 34%.

Plain Language Summary Climate change is induced by gases like carbon dioxide, which are added to the atmosphere. The increase of the concentration in the atmosphere is dampened by the uptake of this gas by land and ocean. Especially, the coastal ocean is able to efficiently absorb CO_2. To calculate the North Sea-wide uptake of CO_2, simulated wind speed data were used. The formerly used model data cover the total Earth and thus have a less fine resolution. Especially near the coast this effect becomes dominant, as wind over land is more efficiently retarded than over sea. A new wind product (coastDat) with a refined grid was established especially for coastal applications. We compare the old and the new data with observational data sets. It has shown that the coastDat data are closer to observations near the coast. The old data set significantly underestimates the observational data there. At the open sea the new data set slightly overestimates the observations. The comparison of the mean flux of CO_2 from the atmosphere into the ocean revealed an increase of 34% when using the new wind data instead of the old one.

1. Introduction

Carbon fluxes in coastal and shelf seas are highly variable at various spatial and temporal scales. This high variability is caused by exchanges of matter and energy between these marine environments and the adjacent Earth system compartments land, open ocean, atmosphere, and shallow sediments. Furthermore, primary productivity in coastal and shelf seas is one of the highest of all marine environments, and consecutive respiratory processes regulate the carbon cycle at seasonal to annual time scales. The high primary productivity is fueled by both autochthonous nutrients and nutrient inputs from all the above mentioned neighboring compartments. This eventually yields high aerobic and anaerobic respiratory activity, which further is supported by allochthonous organic matter. Freshwater runoff, heat fluxes, wind, tidal dynamics, and the open ocean regulate circulation and turbulence patterns in coastal and shelf seas, the hydrodynamic foundation of the biogeochemical processes. In synergy, physical and biogeochemical processes govern the CO_2 air-sea exchange, and the interplay of these processes reveals specific characteristics for different coastal and shelf seas (Borges, 2005; Chen & Borges, 2009). As a result, it has been difficult, so far, to establish more reliable, generalized analytical and predictive tools to describe and assess carbon fluxes in these marine environments.

The North Sea, located at the NW European shelf, has been studied extensively during the last two decades, employing both observational and modeling tools. The recent studies have been based largely on a basin-wide field data set with seasonal resolution, gathered in 2001/2002 and consecutive years (e.g., Bozec et al., 2006; Thomas et al., 2004, 2005, 2009) as well as dedicated studies in the southern North Sea (e.g., Schiettecatte et al., 2007). It has been found that, briefly spoken, the North Sea can be subdivided into two biogeochemical regimes, a shallower and permanently mixed southern part and the deeper, stratified northern part (Artioli et al., 2012; Bozec et al., 2005; Große et al., 2016; Kühn et al., 2010; Prowe et al., 2009; Thomas et al., 2004). The northern part constitutes a strong sink for atmospheric CO_2, as CO_2 is exported via the continental shelf pump (Tsunogai et al., 1999) to the deeper Atlantic Ocean (Thomas et al., 2004; Wakelin et al., 2012). In the southern part production and respiration of organic matter occur within the same compartment and their impacts largely cancel out each other, such that resulting net effects on CO_2 air-sea exchange are only moderate (Burt et al., 2016; Prowe et al., 2009; Schiettecatte et al., 2007; Thomas et al., 2004). Furthermore, in the southern part anaerobic respiration in the shallow sediments release alkalinity, which buffers respiratory CO_2 release and causes some parts of the southern North Sea to absorb CO_2 from the atmosphere (Burt et al., 2014, 2016; Thomas et al., 2009). Repeated observations in 2005, 2008, and 2011 have facilitated insights in interannual variability, which is controlled by a complex ramification of the local effects of "weather" patterns and larger-scale climatic pattern primarily governed by the North Atlantic Ocean and the North Atlantic Oscillation (Clargo et al., 2015; Lorkowski et al., 2012; Omar et al., 2010; Salt et al., 2013; Thomas et al., 2007).

Detailed seasonal investigations of CO_2 fluxes between the North Sea and the atmosphere have been reported to reflect the bifurcation of the North Sea (Thomas et al., 2004, 2005) and to be on the order of 1.38 mol $CO_2 \cdot m^{-2} \cdot yr^{-1}$ into the North Sea, with, as mentioned above, the northern part constituting a strong CO_2 sink and the southern part playing a minor or indifferent role with respect to the CO_2 air-sea exchange. This flux assessment has been reported with a range of uncertainty resulting from the reliance on different parametrizations of the CO_2 air-sea transfer coefficient, which overall has been estimated to contribute an approximate of 20% uncertainty to such computations (Watson et al., 2009). As summarized by Wanninkhof (2014) during the recent decade detailed studies have been carried out to further reduce the uncertainty related to the CO_2 air-sea transfer coefficient.

Even though on the global (Shutler et al., 2016), the Atlantic-wide and the regional-scale (Wrobel & Piskozub, 2016) substantial improvements toward the determination of realistic air-sea fluxes (ASF) have been achieved, flux assessments in coastal and shelf seas remain a particular challenge, as the spatial and temporal resolution of environmental data such as wind fields and heat flux data are not necessarily fully adequate to account for the high variability and complexity of these systems (Garbe et al., 2014; Winterfeldt et al., 2011). For example, substantial improvements of heat flux estimates in coastal seas have been achieved by using high-resolution refined meteorological fields (Geyer, 2014). Furthermore, as compared to the off-line integration of modeled data (streams) from different Earth system compartments, the real-time coupling of meteorological and hydrodynamic models has facilitated a more realistic description of temperature and heat flux fields in coastal seas, as, for example, reported for the North Sea by Su et al. (2014).

Largely unknown is the effect of applying refined high-resolution wind fields to the computation of CO_2 ASF in coastal areas, replacing the rather conventional data products from global meteorological fields such as National Centers for Environmental Prediction (Kalnay et al., 1996) or ERA40 by the European Centre for Medium-Range Weather Forecasts (2005). In this study we employ high-resolution wind fields by coastDat (Geyer, 2014), compare those to observational wind data records, and recompile the CO_2 flux assessment for the North Sea by Thomas et al. (2004) using different gas-transfer velocity parameterizations (Wrobel & Piskozub, 2016) in order to investigate in depth the consequences, benefits, and improvements of employing refined high-resolution meteorological forcing when computing CO_2 fluxes in coastal areas.

2. Methods and Data

Throughout this study positive ΔpCO_2 values imply supersaturation of the ocean and negative values indicate undersaturation. Positive ASF represent oceanic uptake of CO_2 and negative fluxes stand for outgassing.

 10.1029/2017JG004281

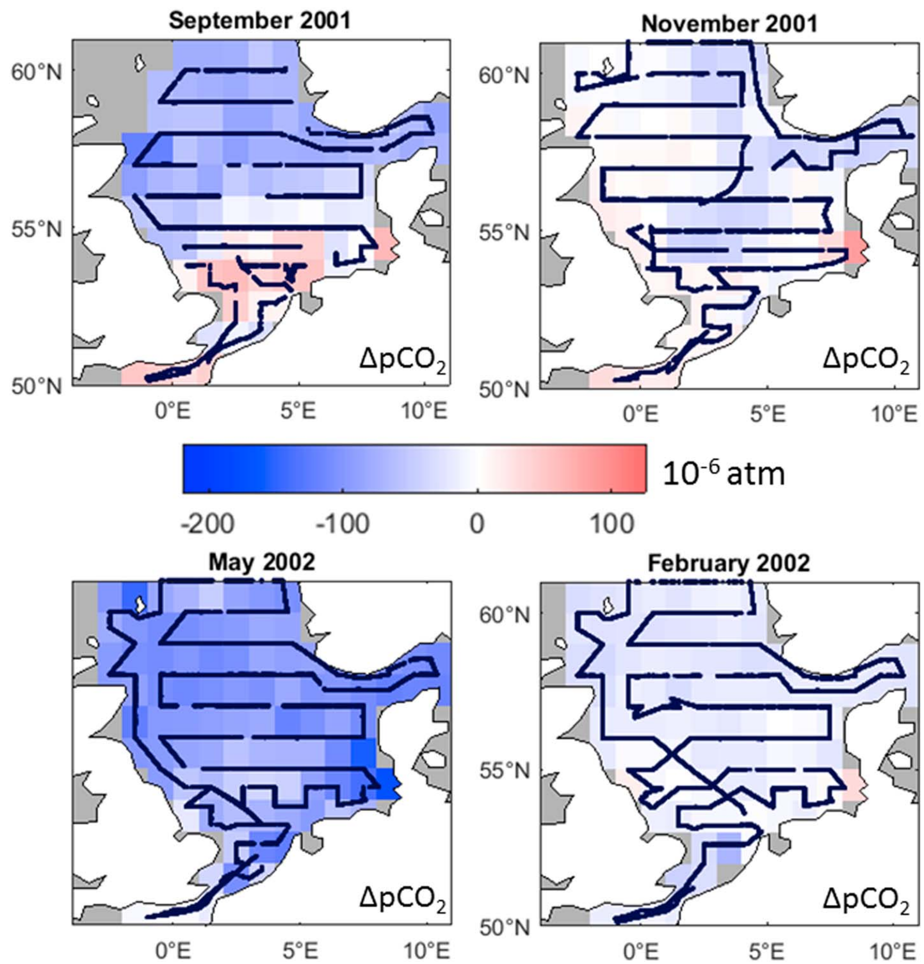

Figure 1. Monthly mean pCO_2 differences (10^{-6} atm) between ocean and atmosphere on the regular 1° × 1° grid derived from measurements. Negative values indicate oceanic undersaturation, positive values indicate supersaturation. Black lines show the course of the cruises.

2.1. The ΔpCO_2 Data

Figure 1 shows the distribution of ΔpCO_2 for September and November 2001 and for February and May 2002 on a 1° × 1° grid together with the corresponding cruise tracks. ΔpCO_2 (μatm) is the difference between marine and atmospheric partial pressure of CO_2. The data were collected on four different cruises with high spatial resolution representing four seasons (Thomas et al., 2004). The summer is represented by the data as the so-called "September values." They were taken from 20 August to 10 September.

For each of the measuring months a complete North Sea-wide field of 1° × 1° cells was established. The cells represent the average of the observational data falling in the respective month and cell. Each observational data is assigned to only one 1° × 1° cell. In case the position data match cell edges the northern or eastern corresponding cell is assigned. The intracell variability, expressed as standard deviation, ranged from 0.26 μatm (northern boundary, November) to 57.6 μatm (off the Danish coast, May). Cells, which could not be filled with data within a specific month, were later handled by horizontal linear interpolation between neighboring cells.

The data are deposited in the PANGAEA data base:

1. https://doi.pangaea.de/10.1594/PANGAEA.610090 (September 2001)
2. https://doi.pangaea.de/10.1594/PANGAEA.610091 (November 2001)
3. https://doi.pangaea.de/10.1594/PANGAEA.610092 (February 2002)
4. https://doi.pangaea.de/10.1594/PANGAEA.610093 (May 2002).

10.1029/2017JG004281

2.2. ERA40

The ERA40 reanalysis data set was established by the European Centre for Medium-Range Weather Forecast in collaboration with other institutes (European Centre for Medium-Range Weather Forecasts, 2005). From this data set we extracted 6-hourly wind components (parameters 165 and 166) and calculated 6-hourly wind speed values (m/s). The original data were interpolated from a 1.25° × 1.25° grid to a regular 1° × 1° grid using the reciprocal of the squared distance to neighboring grid cell centers of the original ERA40 grid. These data were used by Thomas et al. (2004) and in this study.

2.3. coastDat

The coastDat data sets were produced to give a consistent and homogeneous database mainly for assessing weather statistics and climate changes since 1948 for Europe, especially in data sparse regions. The principles of the early data set coastDat2 were defined in Geyer and Rockel (2013). The simulation results used in this study (coastDat3) following these principles were driven by ERAinterim data (Berrisford et al., 2011) and started in 1979. We used hourly output of the nonhydrostatic regional climate model COSMO-CLM version 5.0 for the years 2001 and 2002.

The original data with a spatial resolution of 0.11° in rotated coordinates were converted to the WGS84 regular grid with a resolution of 0.25°. The overall quality of the wind speed data was analyzed by comparison with buoy and quikSCAT data (Geyer, 2014). Especially for near coast applications the data set shows an added value in respect to wind speed statistics (Geyer et al., 2015). For this application the data were further interpolated on a 1° × 1° grid.

The data are deposited in the CERA database:

https://cera-www.dkrz.de/WDCC/ui/Entry.jsp?acronym=coastDat-3_COSMO-CLM_ERAi

2.4. CO_2 Air-Sea Flux Parameterizations

In order to compare the CO_2 flux uncertainty due to different wind products with the uncertainty due to different bulk air-sea flux formulas, we calculate the annual CO_2 fluxes using

1. L&M 1986 (Liss & Merlivat, 1986)
2. T 1990 (Tans et al., 1990)
3. W 1992 (Wanninkhof, 1992)
4. W&McG 1999 (Wanninkhof & McGillis, 1999)
5. N 2000 (Nightingale et al., 2000)
6. W 2014 (Wanninkhof, 2014)

In the following W&McG 1999 was applied if not stated otherwise. The W 1992 formula is used among the others even though it is known that it is problematic (Wanninkhof, 2014). It is applied here for comparison with the results of Thomas et al. (2004).

2.5. Height Correction of Observed Wind Speed

Wind speed is corrected to a height of 10 m above the sea surface using equation (1) of Sutton et al. (2017).

$$U_{10} = \frac{U_z}{1 + \frac{\sqrt{Cd_{10}}}{0.4} \times \ln\left(\frac{z}{10}\right)}$$

where U_{10} is wind speed in m/s at 10 m, z is the height (m) of the wind sensor, U_z is wind speed in m/s recorded by the sensor, Cd_{10} is the drag coefficient (0.0011), and 0.4 is von Karman constant.

3. Results

3.1. Comparison of Wind Data

Figure 2 shows the horizontal distributions of differences of the mean wind fields derived from ERA40 and coastDat for the months September and November 2001 and February and May 2002. For most cases the coastDat values are larger than the corresponding ERA40 values. For all months but May almost all nearshore differences are high (2 m/s or larger). In the Skagerrak highest differences (>4 m/s) appear in November and February. In May a large area in the central North Sea shows very small differences. During the other months the differences are there in the range of 0.5–1 m/s.

10.1029/2017JG004281

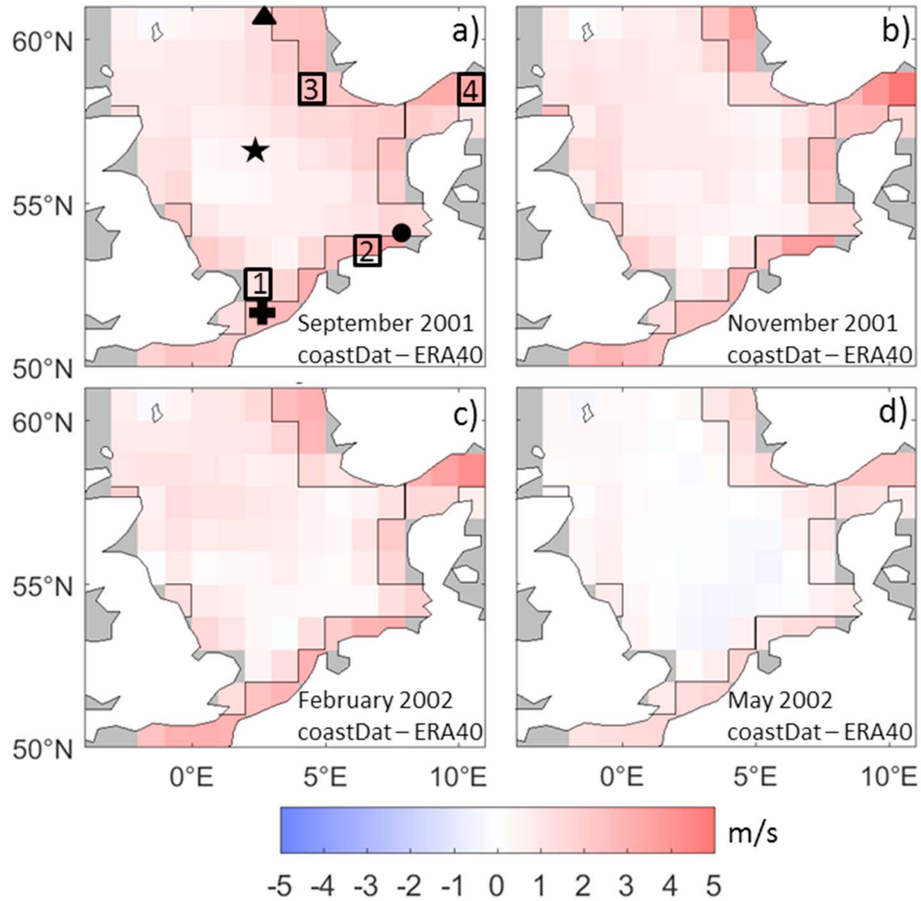

Figure 2. Monthly mean wind speed difference (coastDat − ERA40; m/s) on the regular 1° × 1° grid. The black polygons indicate coastal areas with wind speed differences larger than 2 m/s at least once during the shown months. Figure 2a - September 2001 with the positions of four cells indicated by rectangles, the position of the observational stations: Troll = triangle; Ekofisk = asterisk; Helgoland = dot; Westhinder = cross. Figure 2b - November 2001; Figure 2c - February 2002; Figure 2d - May 2002 data.

The spatial variability of the 1° × 1° wind fields for 4 months is shown as mean (6 hr) standard deviations (σ) in Table 1. The last column, the mean of the relative standard deviations, shows that both wind products bear more or less the same relative spatial variabilities.

To evaluate the temporal development of the different wind data, the time series of 6-hourly wind speeds derived by coastDat and ERA40 were compared for four different 1° × 1° grid cells for September 2001 (Figure 3). Table 2 gives corresponding statistical data.

Obviously, the data of the two products are in phase regarding to the variability of periods larger than 2–3 days. For all cells considered, the means and the standard deviations of the coastDat data are larger than

Table 1
Monthly Means of Horizontal Wind Speed Averages (μ) and Standard Deviations (σ) of the 1° × 1° Cells

	September 2001		November 2001		February 2002		May 2002		
(m/s)	μ	σ	μ	σ	μ	σ	μ	σ	$\overline{\sigma/\mu}$
ERA40	6.99	2.41	8.41	2.69	9.68	2.96	6.55	2.06	0.32
coastDat	8.34	2.72	9.78	2.74	10.91	3.10	7.05	2.39	0.31

Note. The last column gives the mean of the relative standard deviations.

10.1029/2017JG004281

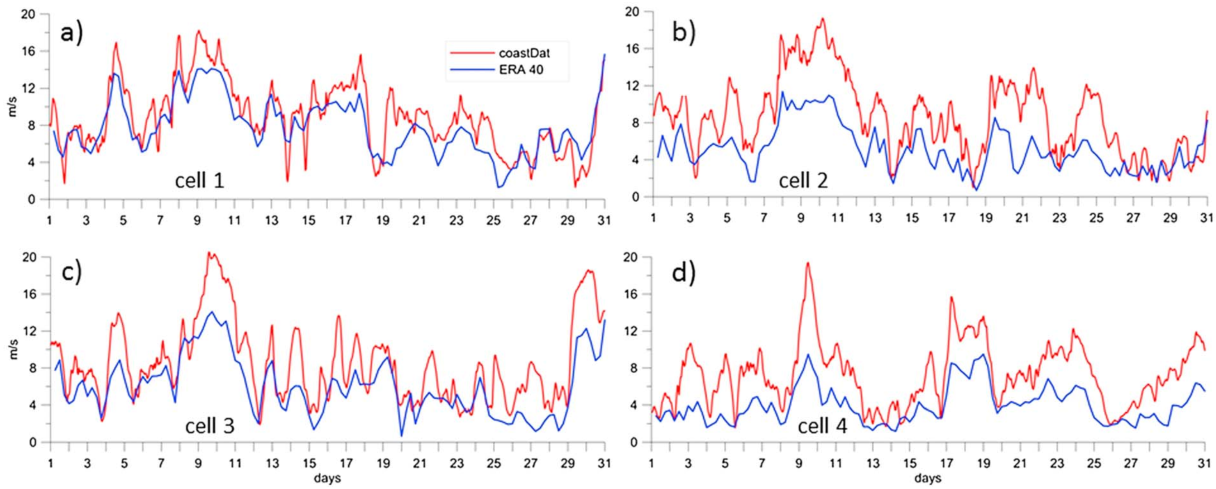

Figure 3. Time series of ERA40 and coastDat wind speed for 4 different cells in September 2001. The position of the cells are defined in Figure 2a and Table 2.

the corresponding ERA40 data. This effect is strongest for cell 4 in the Skagerrak. A rather strong deviation can also be seen for cell 3 off the Norwegian coast.

Figure 4 displays the area-weighted North Sea-wide monthly averages of the wind speed for both sources, ERA40 and coastDat. Highest values fall in February, lowest in July, where the strongest relative deviation between the two products occur (15.1%).

In addition, we compared the two data sets with observational data from the DWD (DWD Climate Data Center, 2016) at Helgoland in the German Bight (54.175°N, 7.892°E). For comparison we used ERA40 and coastDat data of the corresponding 1 × 1° grid cell. The use of corresponding 0.25 × 0.25 grid cell of coastDat did not improve the comparison. The observational data are hourly averages of wind speed 10 m above ground, the ERA40 data represent more or less instantaneous values, and the coastDat data are recorded hourly instantaneously. We used the representation of hourly data and interpolated the ERA40 data to hourly values. Figure 5 illustrates the overall agreement in phase and amplitude. In most cases the mean and standard deviation of the ERA40 data are lower than the corresponding coastDat and observational data. This is also confirmed by the insert tables showing statistical values for the different months. The means and the standard deviations in May 2002 are significantly lower than those in the other months, whereas highest values appear in February 2002. In some cases the peak values of the coastDat data overestimate the amplitudes of the observations.

At the Westhinder platform off the Belgium coast (51.39°N, 2.44°E) 10 min wind speed averages were measured 23.85 m above ground. These data were acquired by the Meetnet Vlaamse Banken and retrieved from the AGENTSCHAP MARITIEME DIENSTVERLENING en KUST (http://www.vliz.be/vmdcdata/midas/MVBgraph.php). From this product we calculated the hourly averaged U10 wind speed (10 m above ground; Figure 6). The comparison of these observational data with ERA40 values shows, similar to the Helgoland comparison, a general underestimation of the observations. The monthly averages of the ERA40 time series are about 2–3 m/s lower than the corresponding observational averages (insert tables). Also, the standard deviation is significantly lower. The coastDat data are much closer to the observations, but the monthly averages slightly underestimate them.

Table 2
Means (μ) and Standard Deviations (σ) of 6-Hourly Wind Data for coastDat and ERA40 at Four Cells in September 2001 and the Relative Standard Deviations (σ/μ)

(m/s)	Longitude	Latitude	ERA40 μ	coastDat μ	ERA40 σ	coastDat σ	ERA40 σ/μ	coastDat σ/μ
Cell 1	2.5°E	52.5°N	7.75	8.86	3.03	3.63	0.39	0.41
Cell 2	6.5°E	53.5°N	5.13	8.59	2.43	4.05	0.47	0.47
Cell 3	4.5°E	58.5°N	6.02	8.53	3.17	4.26	0.53	0.50
Cell 4	10.5°E	58.5°N	3.99	7.28	1.99	3.36	0.50	0.46

Note. The positions of the 1° × 1° cells identify the cell centers and are shown in Figure 2a.

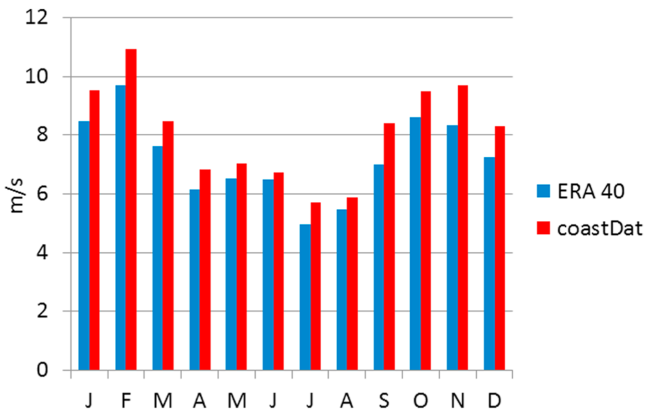

Figure 4. Area-weighted North Sea-wide monthly averages of the wind speed for ERA40 and coastDat.

Thanks to the Norwegian Meteorological Institute it was possible to compare the two wind products with observations from two different Norwegian oil platforms (www.eklima.no). Both stations delivered 20-min averages of wind speed 10 m above ground, which was calculated to hourly averages. For the more northern platform Troll (60.64°N, 3.72°E) only data for 2002 were available. In most cases (Figure 7) phase and amplitude are coherent for all data, but in February some of the coastDat values overestimate the observations. Consequently, the monthly February mean is higher than the mean of the observational data (insert tables). The platform Ekofisk in the central North Sea (56.54°N, 3.22°E) delivered data for all four months (Figure 8). Phase and amplitude for all three data sets are in most cases coherent. For all months but May the monthly averages are overestimated by coastDat, whereas the ERA40 data are closer to observational means.

3.2. Annual ASF of CO_2

For calculating the North Sea-wide annual fluxes of CO_2 the four measurement-derived fields of ΔpCO_2 values for the months February, May, September, and November were cell-wise temporally linearly interpolated (Jiang et al., 2008). Other temporal interpolation methods and the consequences for the resulting ASF are discussed in section 4.3. The monthly values are treated as representative for both years and were used to reproduce a yearly cycle. The results were monthly ΔpCO_2 fields. Figure 9a shows the annual cycle for the four cells indicated in Figure 2a and Table 2: Only cell 1 in the south exhibits positive values. They fall in the time between July and November. All other cells show negative values indicating undersaturation of the ocean.

The summer and early fall CO_2 efflux at cell 1 is representative for parts of the southern North Sea (Figure 1). Responsible for this flux is the relative high temperature in this area, which reduces the solubility of dissolved

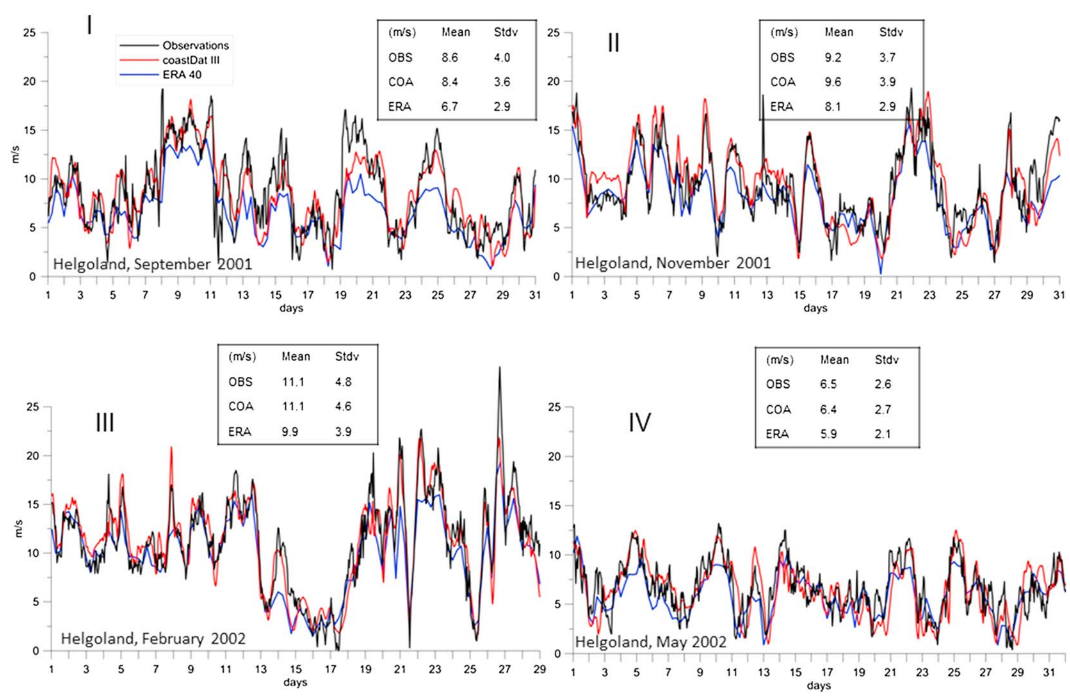

Figure 5. Time series of hourly averaged wind speed at Helgoland (54.175°N, 7.892°E) for (I) September 2001, (II) November 2001, (III) February 2002, and (IV) May 2002 using simulated ERA40 and coastDat values in comparison with observations. The 6-hourly ERA40 data were linearly interpolated to hourly values. The insert tables give means and standard deviations for the different time series.

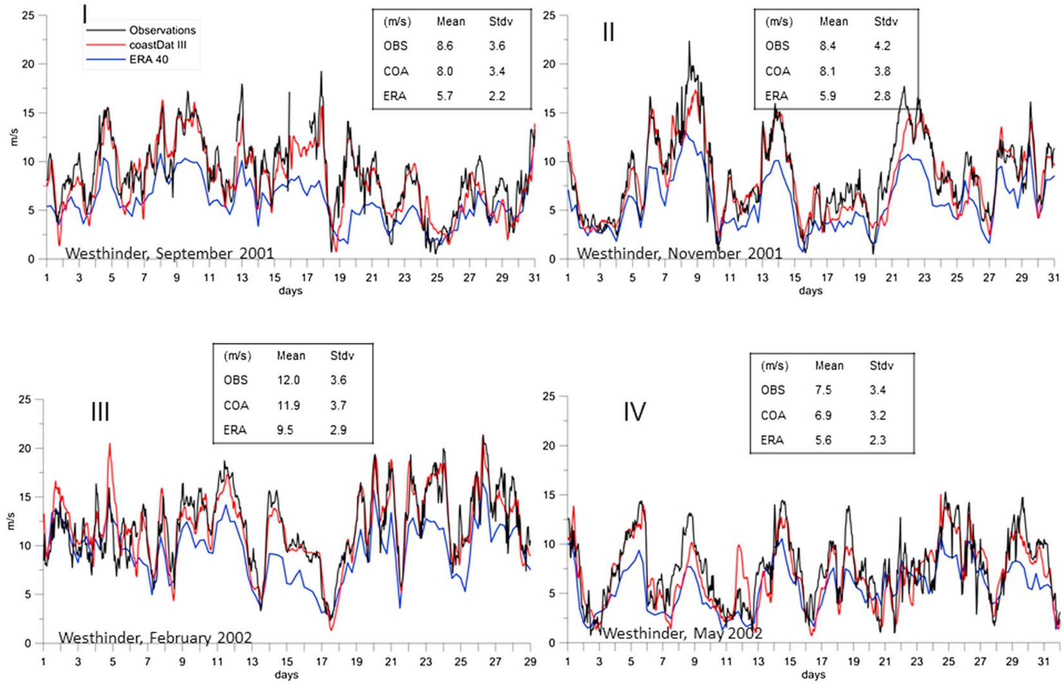

Figure 6. Time series of hourly averaged wind speed at Westhinder (51.39°N, 2.44°E) for (I) September 2001, (II) November 2001, (III) February 2002, and (IV) May 2002 using simulated ERA40 and coastDat values in comparison with observations. The 6-hourly ERA40 data were linearly interpolated to hourly values. The insert tables give means and standard deviations for the different time series.

gases in the water. Kühn et al. (2010) were able to discriminate the biological and the physical carbon pump of the southern North Sea on a seasonal basis (their Figure 5c). They found an overall outgassing between summer and early fall, which was mainly caused by nonbiological mechanisms and a concurrently small uptake of atmospheric CO_2 due to net biological activities.

Using the bulk formulas by Wanninkhof and McGillis (1999), the monthly ΔpCO_2 values, and the wind data, we calculated monthly means of CO_2 ASF for each of the $1° \times 1°$ cells. Figure 9b shows the annual cycle of these fluxes for the chosen cells when using ERA40 data and Figure 9c shows the corresponding fluxes under the use of coastDat data. In most cases the coastDat-driven fluxes are larger than those driven by ERA40. This is clearly induced by the generally higher wind speeds of the coastDat data set.

The seasonal cycle of the North Sea-wide net CO_2 fluxes is shown in Figure 10. Largest fluxes can be found during the time when biological production dominates organic matter degradation in March to June

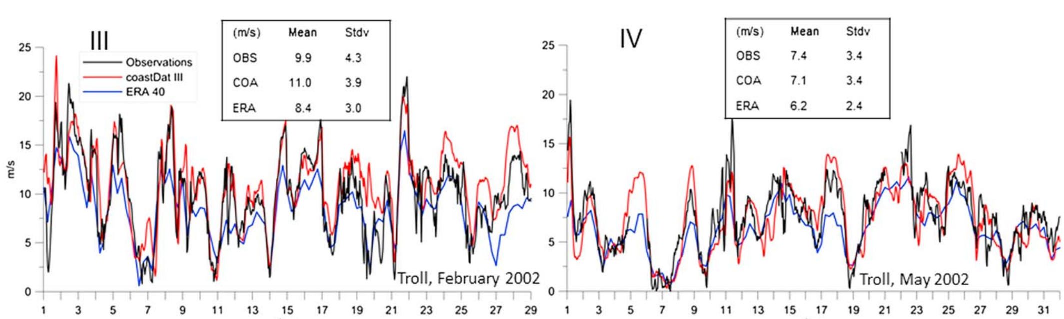

Figure 7. Time series of hourly averaged wind speed at the oil platform Troll (60.64°N, 3.72°E) for (III) February 2002, and (IV) May 2002 using simulated ERA40 and coastDat values in comparison with observations. The 6-hourly ERA40 data were linearly interpolated to hourly values.

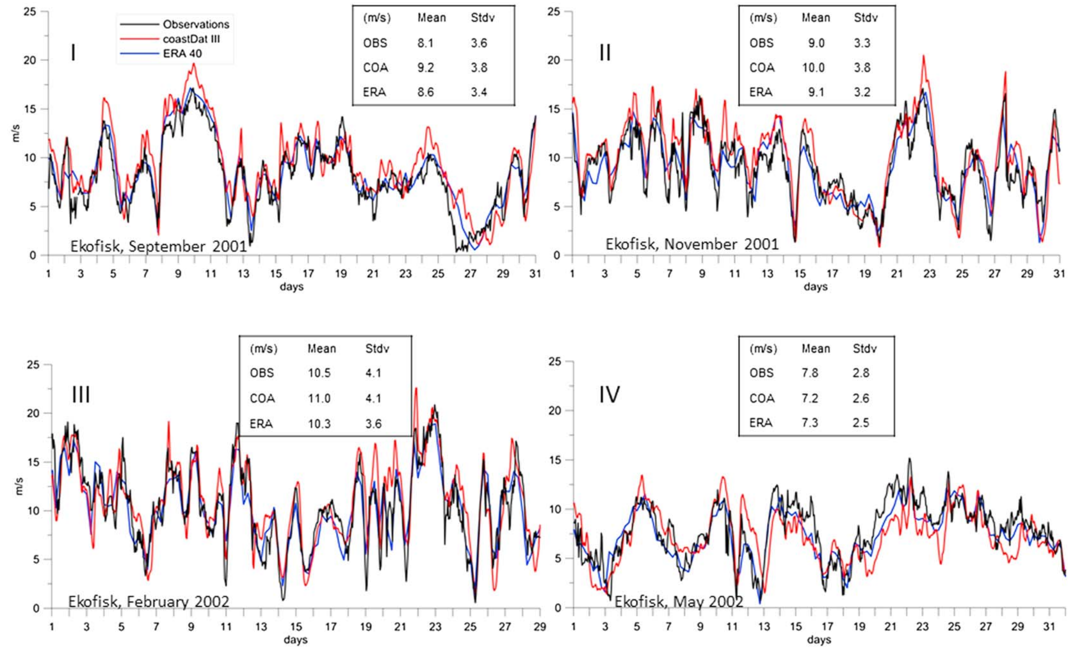

Figure 8. Time series of hourly averaged wind speed at the oil platforms Ekofisk at (56.54°N, 3.22°E) for (I) September 2001, (II) November 2001, (III) February 2002, and IV) May 2002 using simulated ERA40 and coastDat values in comparison with observations. The 6-hourly ERA40 data were linearly interpolated to hourly values.

(compare Kühn et al., 2010, their Figure 5a). During this time also largest absolute deviations between coastDat and ERA40 derived fluxes occur.

Figure 11 shows the horizontal distribution of the flux differences. Highest differences appear off the Norwegian coast where also the differences in wind speed were largest (Figure 2).

The small deviation between the ERA40-based estimation of the annual CO_2 ASF of Thomas et al., 2004 (1.38 $mol \cdot m^{-2} \cdot yr^{-1}$) and of this study (1.49 $mol \cdot m^{-2} \cdot yr^{-1}$) can be explained by the different interpolation methods of the ΔpCO_2 measurements into 13 boxes (Thomas et al., 2004) and into 1° × 1° cells (this study). But even when the method by Thomas et al. (2004), who aggregated the observations into 13 large boxes, was adopted, a deviation of the overall annual flux (1.28 $mol \cdot m^{-2} \cdot yr^{-1}$) remained. This is due to the fact that we used area weighted 1° × 1° cells to fill the individual large boxes.

In literature several bulk formulas for calculating the ASF of CO_2 exist: Liss and Merlivat (1986) and Tans et al. (1990) prescribe a linear relationship between flux and wind speed. Quadratic relations were used by Wanninkhof (1992), Nightingale et al. (2000), and Wanninkhof (2014), while a cubic relation was used by Wanninkhof and McGillis (1999). Figure 12a shows the North Sea-wide net annual fluxes using the different bulk fluxes and the different wind products. Highest fluxes were produced by the formula by Tans et al. (1990). The strongest deviation (34%) between the fluxes driven by the different wind products is achieved by the cubic approach by Wanninkhof and McGillis (1999). When evaluating the gross annual fluxes (Figure 12b) the maximum deviation is even larger (39%). In this context gross annual fluxes are the sum of the hourly absolute values of the fluxes.

4. Summary and Discussion

4.1. Wind Data Products

The comparison of the two data sets suggests that ERA40 data are in most cases lower than the coastDat data. This is in line with the conclusions by Brodeau et al. (2010), who found that the global surface winds are underestimated by ERA40. The areas with the largest deviations between the two data sets are the continental coast, the Norwegian wider coast, and the Skagerrak. The latter two areas are also highlighted by Winterfeldt et al. (2011) and Geyer et al. (2015) as areas showing highest added values comparing the

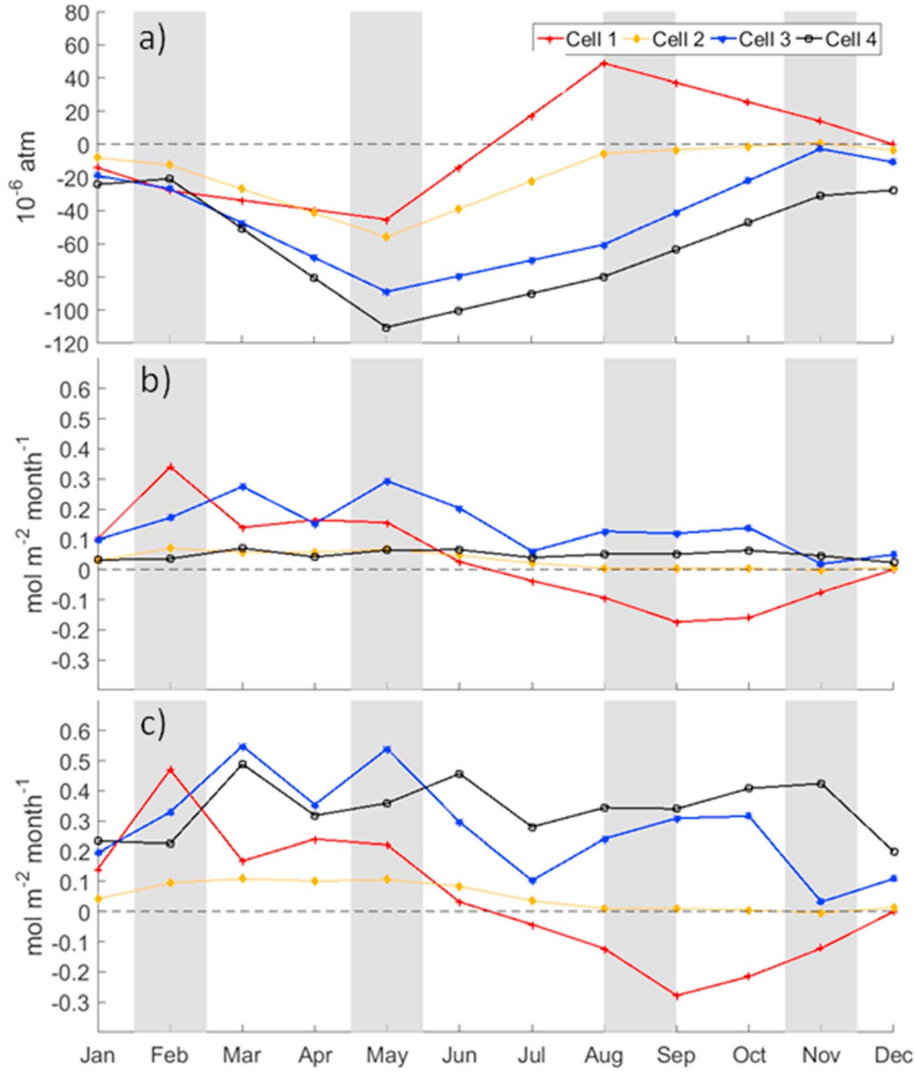

Figure 9. Time series of monthly mean (a) ΔpCO_2 values, (b) CO_2 fluxes using ERA40 wind data, and (c) CO_2 fluxes using coastDat wind data. The gray shaded areas indicate the time of observations. Positive fluxes imply marine uptake of atmospheric CO_2.

globally simulated and the regional downscaled wind fields. Comparing observational and wind product data at Helgoland and Westhinder, the larger values of coastDat appear justified. Relative to observed wind data derived from Norwegian platforms, coastDat data reveal a moderate overestimation. Especially in the central North Sea at station Ekofisk the peak values (>15 m/s) show overshootings, while at lower wind speeds the data agree well.

4.2. Fluxes of CO_2

4.2.1. Coastal Versus Open Ocean Areas

The largest deviations between coastDat and ERA40 derived CO_2 fluxes should occur in areas where the wind speeds of the different wind products exhibit largest differences and ΔpCO_2 show highest amplitudes. Areas with largest wind differences over the year are coastal areas, which are identified by the black lines in Figure 2. This black line includes cells where the wind difference was at least once in the shown months larger than 2 m/s. The largest ΔpCO_2 amplitudes are negative and match only in May some areas with high wind differences (Figure 2). In May and September large areas with strong negative ΔpCO_2 amplitudes are situated offshore and in the central and northern part of the North Sea where biological production takes place in the upper water column and separated from the upper ocean organic matter is remineralized in

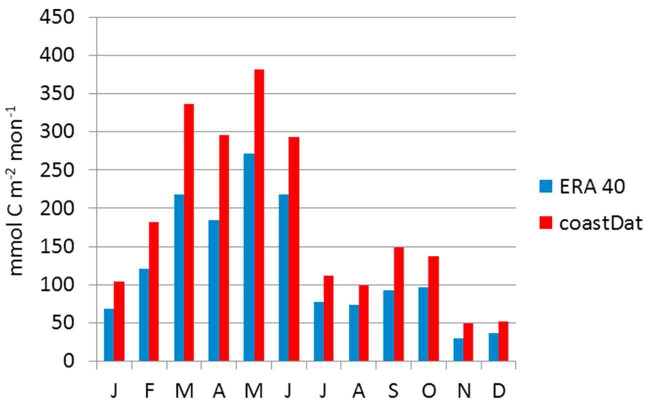

Figure 10. Monthly averages of the North Sea-wide net CO_2 fluxes for ERA40 and coastDat.

the deeper parts (Figure 2). Nevertheless, in those coastal areas where the wind speed differences were larger than 2 m/s (see Figure 2) the net uptake was 0.72 and 1.60 mol C·m^{-2}·yr^{-1} for the application of ERA40 and coastDat, respectively. This means that in coastal areas where vertical mixing dampens strong ΔpCO_2 amplitudes at the surface the choice of the wind product is still crucial.

4.2.2. Different Bulk Formulas of CO_2 Transfer Parameterization

Jiang et al. (2008) listed for all CO_2 transfer parameterizations they used the nonlinearity corrected equations for gas transfer velocities (their Table 3). In our case it is not necessary to introduce nonlinearity coefficients as the sampling rate is 6 hr for ERA40 and 1 hr for coastDat wind data. Nevertheless, Table 3 gives the equations for the gas transfer velocities used in this study.

The uncertainties related to the choice of the bulk formulas are larger than found by Watson et al. (2009). The largest net annual flux (T 2000: 2.35 mol C·m^{-2}·yr^{-1}) is 1.47 times larger than the smallest flux (L&M 1986: 1.6 mol C·m^{-2}·yr^{-1}). This results in a relative deviation of 47%, in case of gross annual fluxes it is 49%. This might have to do with the choice of the six bulk formulas in this study in comparison to the choice of (only) the three formulas used by Watson et al. (2009). Another reason for the deviation is the different study area: While Watson et al. (2009) investigated fluxes of the open North Atlantic with moderate ΔpCO_2 values, the fluxes of the North Sea are more pronounced due to stronger biological activity and a stronger seasonal cycle of the sea surface temperature.

Taking the mean (2.01 mol C·m^{-2}·yr^{-1}) and standard deviation (0.31 mol C·m^{-2}·yr^{-1}) of the net annual fluxes the relative uncertainty amounts to 15.2%, which is even larger than the deviations Vandemark et al. (2011) found for their monthly fluxes when applying different transfer parameterizations (12%). This different findings can be explained by the use of L&M 1986 and T 1990 representing the minimum and maximum annual fluxes in our study.

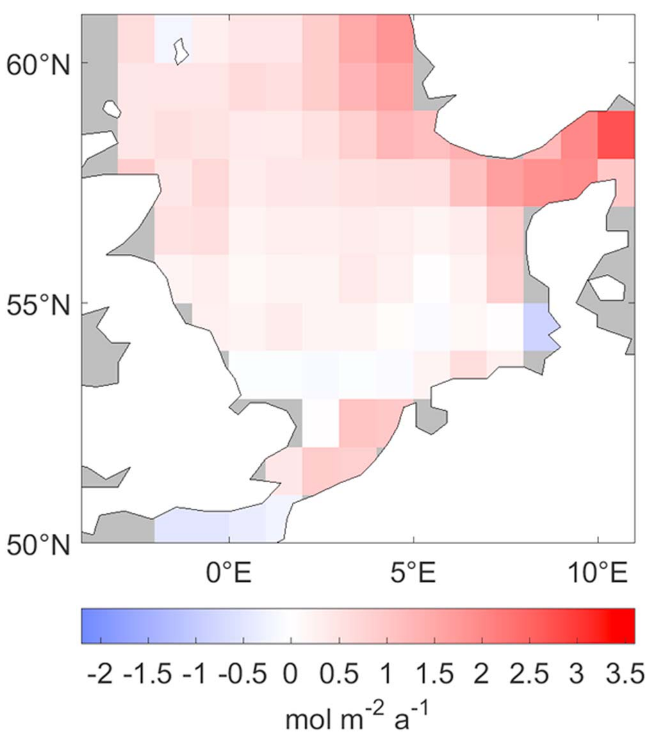

Figure 11. Horizontal distribution of differences of net annual fluxes (coastDat − ERA40).

4.3. Sensitivities of the CO_2 Fluxes

4.3.1. Temporal Interpolation of ΔpCO_2

The observations of ΔpCO_2, temperature and salinity were taken in 4 months of the year only. To calculate annual CO_2 fluxes, the values of the 4 months were interpolated over the year achieving 12 monthly values. For this purpose we interpolated temporally linearly. The annual cycle of ΔpCO_2 is, however, governed by several processes like temperature, mixing, or biological transformations, all highly nonlinear. To investigate the sensitivity of the calculated annual fluxes on the temporal interpolation method, we conducted two additional interpolations:

1. The constant annual average ("const")
2. The stepwise, 3-month constant ("step").

The const interpolation resulted in the highest fluxes: Using coastDat wind fields and the W&Mc 1999 method, the North Sea-wide flux increased by 37%. Especially in winter these fluxes dominated those of the corresponding fluxes derived from linear temporal interpolation.

The step interpolation derived fluxes does not differ strongly from those of the linear interpolation method. Using coastDat wind fields and the W&Mc 1999 method, the North Sea-wide flux decreased by 6%.

4.3.2. Horizontal Resolution of Wind Fields

The potential of the coastDat data is based on the used refined horizontal resolution within the regional climate model COSMO-CLM compared with the corresponding model of the ERA40 data. The subordinated interpolation on a 1° × 1° grid did not change the achieved benefit drastically. This can be seen when comparing near

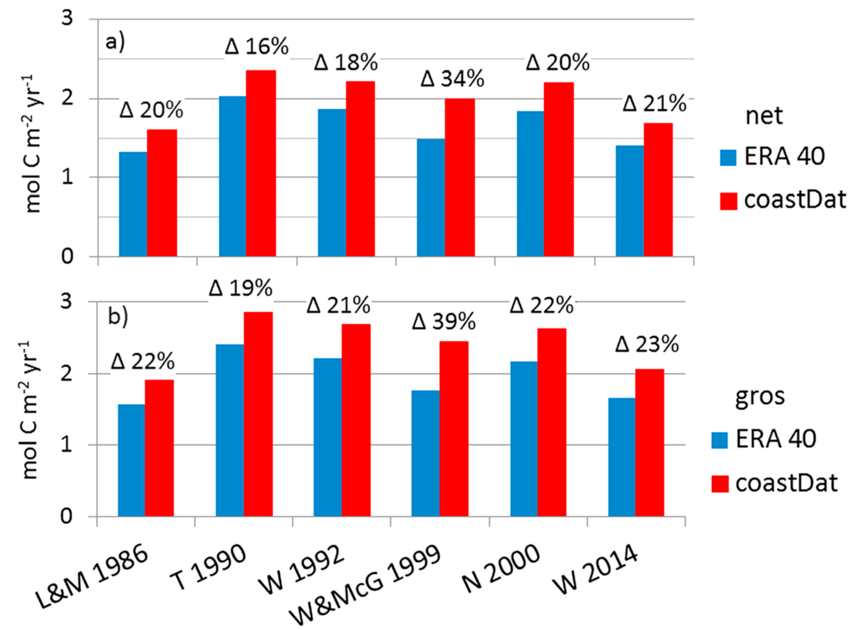

Figure 12. Annual (a) net fluxes and (b) gross fluxes (mol $C{\cdot}m^{-2}{\cdot}yr^{-1}$) for the ERA40 and the coastDat data using different bulk formulas. The percentages indicate the relative deviations between the corresponding fluxes.

coast station data of coastDat, which were extracted from the 1° × 1° (Figures 5 and 6) grid and from the 0.25° × 0.25° grid (Tables 4 and 5). At Helgoland (Table 4) the 1° × 1° means are about 4% larger than the corresponding 0.25° × 0.25° means. This is due to the fact that a large area of the corresponding 1° × 1° cell is situated in the outer German Bight with higher wind speeds than close to the coast (Figure 2a). As can be expected, the temporal variability (σ) of the high-resolution derived values is larger than the variability corresponding to the coarser grid. At Westhinder (Table 5) both the “high-resolution” monthly means and standard variations are larger than those derived from the coarse grid. All deviations are smaller than 4%, which is clearly smaller than the deviations between coastDat and ERA40 at the near coast stations Helgoland and Westhinder (Figures 5 and 6).

In an additional analysis we studied the influence of the grid resolution on annual CO_2 fluxes. In the reference calculation the ΔpCO_2 values and the wind data were interpolated into the 1° × 1° grid, followed by a second step where for each grid cell and month the annual fluxes were calculated (Figure 12). As the coastDat wind product is defined on a 0.25° × 0.25° grid it was possible to use these refined wind data together with the 1° × 1° ΔpCO_2 values to calculate North Sea-wide CO_2 fluxes. In this sensitivity study the mean wind speeds of the 1° × 1° grid cells were the same as in the reference calculation but due to the individual treatment of wind data at the 0.25° × 0.25° grid the annual fluxes increased for all flux parameterizations. The increase was largest (2.7%) for the cubic parameterization W&Mc 1999.

Table 3
Equations for Gas Transfer Velocities for U10 (m/s), the Wind Speed 10 m above ground

Gas transfer velocity (cm/h)	References
$0.17 \cdot U_{10} \quad : \quad U_{10} \le 3.6$ $2.85 \cdot U_{10} - 9.65 \quad : \quad 3.6 < U_{10} \le 13.0$ $5.90 \cdot U_{10} - 49.30 \quad : \quad 13.0 < U_{10}$	L&M 1986
$\frac{0.1825}{\rho \cdot \alpha_s} \cdot (U_{10} - 3) \quad : \quad U_{10} > 3$ $0 \quad : \quad U_{10} \le 3$	T 1990
$\left(0.3 \cdot U_{10}^2\right) \times \left(\frac{Sc}{660}\right)^{-0.5}$	W 1992
$\left(0.0280 \cdot U_{10}^3\right) \times \left(\frac{Sc}{660}\right)^{-0.5}$	W&McG 1999
$\left(0.222 \cdot U_{10}^2 + 0.333 \cdot U_{10}\right) \times \left(\frac{Sc}{660}\right)^{-0.5}$	N 2000
$\left(0.251 \cdot U_{10}^2\right) \times \left(\frac{Sc}{660}\right)^{-0.5}$	W 2014

Note. ρ [kg/l] is the density of seawater, α_s [mol/(kg·atm)] is the solubility of CO_2 in seawater, and Sc is the Schmidt number.

5. Conclusions

The aim of this study is to revise the earlier estimated seasonal resolved annual ASF of CO_2 in the North Sea region (Thomas et al., 2004). This revision mainly focuses on the wind fields, which are used to calculate the gas transfer velocities. The earlier flux estimates were based on 6-hourly ERA40 wind fields originally defined on a 1.25° × 1.25° grid. The new coastDat wind fields used in this study stem from a downscaling experiment of a nonhydrostatic regional model with much higher spatial and temporal resolution (usage of 1-hourly and 0.25° × 0.25°

Table 4
Monthly Means (μ) and Standard Deviations (σ) of Simulated coastDat Wind Speeds at Helgoland (See Figure 5) Derived From One Cell of the 1° × 1° Grid and From One Cell of the 0.25° × 0.25° Grid

Helgoland (m/s)	Sep 2001	Nov 2001	Feb 2002	May 2002	Deviation
μ (1° × 1°)	8.44	9.59	11.12	6.42	95.99%
μ (0.25° × 0.25°)	8.02	9.15	10.99	6.08	
σ (1° × 1°)	3.58	3.95	4.56	2.74	103.43%
σ (0.25° × 0.25°)	3.83	3.98	4.80	2.76	

resolution). For comparison with the earlier CO_2 flux estimates we made the following assumptions:

1. As the earlier flux estimate used 1° × 1° cells on which the ERA40 wind fields were interpolated, in this study the coastDat wind data and the corresponding ΔpCO_2 data are also interpolated onto this 1° × 1° field. It could be shown that with the use of these new wind fields the estimate of the net annual CO_2 flux increased by 16–34% depending on the choice of the parameterization of the gas transfer velocity. The direct use of the originally higher resolved wind fields increased the estimated flux additionally by only up to 2.7%. For some regions it would be even possible to better resolve the ΔpCO_2 data, but in this case many grid cells elsewhere would not show any pCO_2 observation (Figure 1), and thus, strong interpolation assumptions would be necessary. To include also near coast or even estuary areas (with assumed substantial deviations from open North Sea ΔpCO_2 values), a synoptic combination of open North Sea and coastal observations would be necessary.
2. As the sampling rate of the wind data was relatively high it was not necessary to apply nonlinearity correction coefficients (Jiang et al., 2008).
3. As each cruise (Figure 1) was conducted continuously no apparent diel variations of the ΔpCO_2 observations should bias the annual flux estimates.
4. Following the argument by Jiang et al. (2008), the cool skin effect was neglected.
5. To calculate diagnostically the CO_2 air-sea flux with different wind data products or different bulk formulas neglects the feedback mechanisms, which dampens overestimations or underestimations of the fluxes by the fact that the seawater stores the carbon and releases or outgasses "erroneously" calculated CO_2 afterward. The implementation of these different techniques within a prognostic biogeochemical model would yield less different CO_2 fluxes as the feedback mechanisms controlling the ΔpCO_2 do not allow unchecked overestimated or underestimated fluxes. Therefore, the given estimated flux differences in this study hold as upper limits discriminating the different techniques and the resulting fluxes.

For most areas the coastDat wind velocities are larger than those of ERA40 (Figure 2). To take this into account, the variability analysis is based on relative standard deviations (σ/μ). While the analysis of the horizontal variability of the two wind fields (on the 1° × 1° grid) show comparable relative standard variations (Table 1), the temporal relative standard deviations (of 6-hourly data) of the more northern ERA40 data are larger than those of the coastDat data, while the southern coastal cells show comparable (relative) variabilities (Table 2).

The strongest impact of the new wind product (coastDat) on CO_2 fluxes is detected in coastal areas. It increases there from 0.72 to 1.60 mol C·m^{-2}·yr^{-1}. The increase at the open sea is 0.35 mol C·m^{-2}·yr^{-1}. According to these numbers, the basin-wide estimate of 1.38 mol C·m^{-2}·yr^{-1} by Thomas et al. (2004) would be replaced by 1.85 mol C·m^{-2}·yr^{-1}. Comparisons of the different wind products with coastal observational data clearly reveal the benefit of the coastDat data in such areas. For the open North Sea such comparisons with observations showed that coastDat wind data overestimate the observational data by 5–10%. In most cases the ERA40 data are closer to the observations. Only in May when the mean velocities are lower than in other months the coastDat wind velocities better represent the observations than ERA40 values. This

Table 5
Monthly Means (μ) and Standard Deviations (σ) of Simulated coastDat Wind Speeds at Westhinder (See Figure 6) Derived From One Cell of the 1° × 1° Grid and From One Cell of the 0.25° × 0.25° Grid

Westhinder (m/s)	Sep 2001	Nov 2001	Feb 2002	May 2002	Deviation
μ (1° × 1°)	7.98	8.15	11.90	6.90	101.57%
μ (0.25° × 0.25°)	8.05	8.29	12.08	7.05	
σ (1° × 1°)	3.40	3.77	3.66	3.21	104.35%
σ (0.25° × 0.25°)	3.51	3.86	3.76	3.50	

may allow the conclusion that for the open North Sea both wind products are suitable to calculate annual ASF of CO_2. In strong wind situations (>8 m/s) the ERA40 data offer a small benefit compared to the coastDat data. In coastal regions the coastDat wind data are clearly more suitable to calculate annual air-sea CO_2 fluxes than the ERA40 wind data.

Ongoing acidification and ocean surface warming increase the ocean partial pressure of CO_2. This could already be shown by repeated observations in 2005 in the North Sea (Thomas et al., 2007). With our data we tested the relative deviations of annual ASF when applying the different wind fields, reduced $\Delta p CO_2$ values (−10 μatm) and increased surface temperatures (+1 °C). For this "future scenario" the relative difference of the annual air-sea fluxes between the coastDat and the ERA40 wind applications were reduced by 2–3% in comparison to the realistic scenario for 2001/2002. This means that in the future suitable $\Delta p CO_2$ values become more important than the further upgrade of wind data quality.

Acknowledgments
This work was supported through the Cluster of Excellence CliSAP (EXC177), University of Hamburg, funded through the German Research Foundation (DFG). We thank Dieter Bürckel, Alberto Borges, Ellen Lenaers, and Henning Wehde for valuable references concerning data retrieval. The pCO_2 data are deposited in the PANGAEA data base: https://doi.pangaea.de/10.1594/PANGAEA.610090 (for Sep 2001), https://doi.pangaea.de/10.1594/PANGAEA.610091 (for November 2001), https://doi.pangaea.de/10.1594/PANGAEA.610092 (for February 2002), and https://doi.pangaea.de/10.1594/PANGAEA.610093 (for May 2002). The observational wind data are available at the following sites: Helgoland: ftp://ftp-cdc.dwd.de/pub/CDC/observations_germany/climate/hourly/wind/historical/, Westhinder: http://www.vliz.be/vmdcdata/midas/MVBgraph.php,%20 and Norway: www.eklima.no. The coastDat data are available at: https://cera-www.dkrz.de/WDCC/ui/Entry.jsp?acronym=coastDat-3_COSMO-CLM_ERAi.

References

Artioli, Y., Blackford, J. C., Butenschön, M., Holt, J. T., Wakelin, S. L., Thomas, H., et al. (2012). The carbonate system in the North Sea: Sensitivity and model validation. *Journal of Marine Systems*, *102-104*, 1–13. https://doi.org/10.1016/j.jmarsys.2012.04.006

Berrisford, P., Kållberg, P., Kobayashi, S., Dee, D., Uppala, S., Simmons, A. J., et al. (2011). Atmospheric conservation properties in ERA-Interim. *Quarterly Journal of the Royal Meteorological Society*, *137*(659), 1381–1399. https://doi.org/10.1002/qj.864

Borges, A. V., Delille, B., & Frankignoulle, M. (2005). Budgeting sinks and sources of CO_2 in the coastal ocean: Diversity of ecosystem counts. *Geophysical Research Letters*, *32*, L14601. https://doi.org/10.1029/2005GL023053

Bozec, Y., Thomas, H., Elkaly, K., & Baar, H. D. (2005). The continental shelf pump in the North Sea—Evidence from summer observations. *Marine Chemistry*, *93*(2-4), 131–147. https://doi.org/10.1016/j.marchem.2004.07.006

Bozec, Y., Thomas, H., Schiettecatte, L.-S., Borges, A. V., Elkalay, K., & De Baar, H. J. W. (2006). Assessment of processes controlling seasonal variations of dissolved inorganic carbon in the North Sea. *Limnology and Oceanography*, *51*(6), 2746–2762. https://doi.org/10.4319/lo.2006.51.6.2746

Brodeau, L., Barnier, B., Treguier, A.-M., Penduff, T., & Gulev, S. (2010). An ERA40-based atmospheric forcing for global ocean circulation models. *Ocean Modelling*, *31*(3–4), 88–104. https://doi.org/10.1016/j.ocemod.2009.10.005

Burt, W. J., Thomas, H., Hagens, M., Pätsch, J., Clargo, N. M., Salt, L. A., et al. (2016). Carbon sources in the North Sea evaluated by means of radium and stable carbon isotope tracers. *Limnology and Oceanography*, *61*(2), 666–683. https://doi.org/10.1002/lno.10243

Burt, W. J., Thomas, H., Pätsch, J., Omar, A. M., Schrum, C., Daewel, U., et al. (2014). Radium isotopes as a tracer of sediment-water column exchange in the North Sea. *Global Biogeochemical Cycles*, *28*, 786–804. https://doi.org/10.1002/2014GB004825

Chen, C.-T. A., & Borges, A. V. (2009). Reconciling opposing views on carbon cycling in the coastal ocean: Continental shelves as sinks and near-shore ecosystems as sources of atmospheric CO_2. *Deep-Sea Research Part II*, *56*(8-10), 578–590. https://doi.org/10.1016/j.dsr2.2009.01.001

Clargo, N. M., Salt, L. A., Thomas, H., & De Baar, H. J. W. (2015). Rapid increase of observed DIC and pCO_2 in the surface waters of the North Sea in the 2001–2011 decade ascribed to climate change superimposed by biological processes. *Marine Chemistry*, *177*(3), 566–581. https://doi.org/10.1016/j.marchem.2015.08.010

DWD Climate Data Center (2016). Historical hourly station observations of wind speed and wind direction, version v004. Retrieved from ftp://ftp-cdc.dwd.de/pub/CDC/observations_germany/climate/hourly/wind/historical/

European Centre for Medium-Range Weather Forecasts (2005). European Centre for Medium-Range Weather Forecasts, Re-Analysis ERA-40 online dataset. Retrieved from https://cera-www.dkrz.de/WDCC/ui/cerasearch/q?hierarchy_steps_ss=ERA40

Garbe, C. S., Rutgersson, A., Boutin, J., de Leeuw, G., Delille, B., Fairall, C. W., et al. (2014). Transfer across the air-sea Interface. In P. S. Liss & M. T. Johnson (Eds.), *Ocean-atmosphere interactions of gases and particles*, *Earth Sys. Sci.* (pp. 55–111). Berlin, Heidelberg: Springer. https://doi.org/10.1007/978-3-642-25643-1_2

Geyer, B. (2014). High-resolution atmospheric reconstruction for Europe 1948–2012: coastDat2. *Earth System Science Data*, *6*(1), 147–164.

Geyer, B. & Rockel, B. (2013). coastDat-2COSMO-CLM.WorldDataCenterforClimate. CERA-DB coastDat-2_COSMO-CLM. Retrieved from http://cera-www.dkrz.de/WDCC/ui/Compact.jsp?acronym¼coastDat-2_COSMO-CLM

Geyer, B., Weisse, R., Bisling, P., & Winterfeldt, J. (2015). Climatology of North Sea wind energy derived from a model hindcast for 1958–2012. *Journal of Wind Engineering and Industrial Aerodynamics*, *147*, 18–29. https://doi.org/10.1016/j.jweia.2015.09.005

Große, F., Greenwood, N., Kreus, M., Lenhart, H. J., Machoczek, D., Pätsch, J., et al. (2016). Looking beyond stratification: A model-based analysis of the biological drivers of oxygen deficiency in the North Sea. *Biogeosciences*, *13*(8), 2511–2535. https://doi.org/10.5194/bg-13-2511-2016

Jiang, L.-Q., Cai, W.-J., Wanninkhof, R., Wang, Y., & Luger, H. (2008). Air-sea CO2 fluxes on the U.S. South Atlantic Bight: Spatial and seasonal variability. *Journal of Geophysical Research*, *113*, C07019. https://doi.org/10.1029/2007JC004366

Kalnay, E., Kanamitsu, M., Kistler, R., Collins, W., Deaven, D., Gandin, L., et al. (1996). The NCEP/NCAR 40-year reanalysis project. *Bulletin of the American Meteorological Society*, *77*(3), 437–471. https://doi.org/10.1175/1520-0477(1996)077%3C0437:TNYRP%3E2.0.CO;2

Kühn, W., Pätsch, J., Thomas, H., Borges, A. V., Schiettecatte, L.-S., Bozec, Y., & Prowe, A. E. F. (2010). Nitrogen and carbon cycling in the North Sea and exchange with the North Atlantic—A model study, Part II: Carbon budget and fluxes. *Continental Shelf Research*, *30*(16), 1701–1716. https://doi.org/10.1016/j.csr.2010.07.001

Liss, P. S., & Merlivat, L. (1986). Air-sea gas exchange rates: Introduction and synthesis. In P. Buat-Menard (Ed.), *The role of air-sea exchange in geochemical cycling* (pp. 113–129). Hingham, MA: D. Reidel. https://doi.org/10.1007/978-94-009-4738-2_5

Lorkowski, I., Pätsch, J., Moll, A., & Kühn, W. (2012). Interannual variability of carbon fluxes in the North Sea from 1970 to 2006—Competing effects of abiotic and biotic drivers on the gas exchange of CO_2. *Estuarine, Coastal and Shelf Science*, *100*, 38–57. https://doi.org/10.1016/j.ecss.2011.11.037

Nightingale, P. D., Liss, P. S., & Schlosser, P. (2000). Measurements of air-sea gas transfer during an open ocean algal bloom. *Geophysical Research Letters*, *27*, 2117–2120. https://doi.org/10.1029/2000GL011541

Omar, A. M., Olsen, A., Johannessen, T., Hoppema, M., Thomas, H., & Borges, A. V. (2010). Spatiotemporal variations of fCO_2 in the North Sea. *Ocean Science*, *6*(1), 77–89. https://doi.org/10.5194/os-6-77-2010

Prowe, A. E. F., Thomas, H., Pätsch, J., Kühn, W., Bozec, Y., Schiettecatte, L.-S., et al. (2009). Mechanisms controlling the air-sea CO_2 flux in the North Sea. *Continental Shelf Research*, *29*(15), 1801–1808. https://doi.org/10.1016/j.csr.2009.06.003

Salt, L. A., Thomas, H., Prowe, A. E. F., Borges, A. V., Bozec, Y., & De Baar, H. J. W. (2013). Variability of North Sea pH and CO_2 in response to North Atlantic Oscillation forcing. *Journal of Geophysical Research: Biogeosciences*, *118*, 1584–1592. https://doi.org/10.1002/2013JG002306

Schiettecatte, L.-S., Thomas, H., Bozec, Y., & Borges, A. V. (2007). High temporal coverage of carbon dioxide measurements in the Southern Bight of the North Sea. *Marine Chemistry*, *106*(1–2), 161–173. https://doi.org/10.1016/j.marchem.2007.01.001

Shutler, J. D., Piolle, J.-F., Land, P. E., Woolf, D. K., Goddijn-Murphy, L., Paul, F., et al. (2016). FluxEngine: A flexible processing system for calculating air-sea carbon dioxide gas fluxes and climatologies. *Journal of Atmospheric and Oceanic Technology*, *33*(4), 741–756. https://doi.org/10.1175/JTECH-D-14-00204.1

Su, J., Yang, H., Pohlmann, T., Ganske, A., Klein, B., Klein, H., & Narayan, N. (2014). A regional coupled atmosphere-ocean model system REMO/HAMSOM for the North Sea KLIWAS Schriftenreihe, KLIWAS--60/2014. https://doi.org/10.5675/Kliwas_60/2014_REMO_HAMSOM

Sutton, A. J., Wanninkhof, R., Sabine, C. L., Feely, R. A., Cronin, M. F., & Weller, R. A. (2017). Variability and trends in surface seawater pCO_2 and CO_2 flux in the Pacific Ocean. *Geophysical Research Letters*, *44*, 5627–5636. https://doi.org/10.1002/2017GL073814

Tans, P. P., Fung, I. Y., & Takahashi, T. (1990). Observational constrains on the global atmospheric CO_2 budget. *Science*, *247*(4949), 1431–1438. https://doi.org/10.1126/science.247.4949.1431

Thomas, H., Bozec, Y., Elkalay, K., de Baar, H. J. W., Borges, A. V., & Schiettecatte, L.-S. (2005). Controls of the surface water partial pressure of CO_2 in the North Sea. *Biogeosciences*, *2*(4), 757–777. https://doi.org/10.1029/JC000571

Thomas, H., Bozec, Y., Elkalay, K., & De Baar, H. J. W. (2004). Enhanced open ocean storage of CO_2 from shelf sea pumping. *Science*, *304*(5673), 1005–1008. https://doi.org/10.1126/science.1095491

Thomas, H., Prowe, A. E. F., van Heuven, S., Bozec, Y., de Baar, H. J. W., Schiettecatte, L.-S., et al. (2007). Rapid decline of the CO_2 buffering capacity in the North Sea and implications for the North Atlantic Ocean. *Global Biogeochemical Cycles*, *21*, GB4001. https://doi.org/10.1029/2006GB002825

Thomas, H., Schiettecatte, L.-S., Suykens, K., Kone, Y. J. M., Shadwick, E. H., Prowe, A. E. F., et al. (2009). Enhanced ocean carbon storage from anaerobic alkalinity generation in coastal sediments. *Biogeosciences*, *6*, 267–274. https://doi.org/10.5194/bg-6-267-2009

Tsunogai, S., Watanabe, S., & Sato, T. (1999). Is there a 'continental shelf pump' for the absorption of atmospheric CO_2? *Tellus*, *51*(3), 701–712. https://doi.org/10.1034/j.1600-0889.1999.t01-2-00010.x

Vandemark, D., Salisbury, J. E., Hunt, C. W., Shellito, S. M., Irish, J. D., McGillis, W. R., et al. (2011). Temporal and spatial dynamics of CO_2 air-sea flux in the Gulf of Maine. *Journal of Geophysical Research*, *116*, C01012. https://doi.org/10.1029/2010JC006408

Wakelin, S. L., Holt, J. T., Allen, J. I., Butenschön, M., & Artioli, Y. (2012). Modeling the carbon fluxes of the northwest European continental shelf: Validation and budgets. *Journal of Geophysical Research*, *117*, C05020. https://doi.org/10.1029/2011JC007402

Wanninkhof, R. (1992). Relationship between wind speed and gas exchange over the ocean. *Journal of Geophysical Research*, *97*, 7373–7382. https://doi.org/10.1029/92JC00188

Wanninkhof, R. (2014). Relationship between wind speed and gas exchange over the ocean revisited. *Limnology and Oceanography: Methods*, *12*(6), 351–362. https://doi.org/10.4319/lom.2014.12.351

Wanninkhof, R., & McGillis, W. R. (1999). A cubic relationship between air-sea CO_2 exchange and wind speed. *Geophysical Research Letters*, *26*, 1889–1892. https://doi.org/10.1029/1999GL900363

Watson, A. J., Schuster, U., Bakker, D. C. E., Bates, N. R., Corbiere, A., Gonzalez-Davila, M., et al. (2009). Tracking the variable North Atlantic sink for atmospheric CO_2. *Science*, *326*(5958), 1391–1393. https://doi.org/10.1126/science.1177394

Winterfeldt, J., Geyer, B., & Weisse, R. (2011). Using QuikSCAT in the added value assessment of dynamically downscaled wind speed. *International Journal of Climatology*, *31*(7), 1028–1039. https://doi.org/10.1002/joc.2105

Wrobel, I., & Piskozub, J. (2016). Effect of gas-transfer velocity parameterization choice on air–sea CO2 fluxes in the North Atlantic Ocean and the European Arctic. *Ocean Science*, *12*(5), 1091–1103. https://doi.org/10.5194/os-12-1091-2016